Impact of reinforcement-concrete interfaces and cracking on gas transfer in concrete

Hognon Sogbossi, Jérôme Verdier, Stéphane Multon

Impact of reinforcement-concrete interfaces and cracking on gas transfer in concrete

Hognon Sogbossi [a], Jérôme Verdier [a], Stéphane Multon [a, 1]

[(a)] *LMDC, Université de Toulouse, INSA, UPS, 135 Avenue de Rangueil, 31077 Toulouse cedex 04 France*

Abstract: The durability of reinforced concrete structures is largely impacted by their transfer properties, which can be evaluated through, for example, permeability measurement. Usually, concrete permeability is studied on plain specimens and the effect of the presence of steel bars on permeability in reinforced concrete has been little studied in the literature. The steel-concrete interface presents a larger porosity than plain concrete, which can be the cause of preferential percolation paths for fluids. Such percolation paths could create a lower resistance to fluid transfer and modify transfer kinetics. For reinforced and prestressed structures with large reinforcement contents, such as found in nuclear power plants, the impact of the reinforcement on gas transfer should be identified to obtain a better assessment of the flow within the structure. The aim of this experimental study is to characterize the effect of the presence of reinforcement on such flows by measuring leakage rates, permeability, and time to reach the steady state**.** Measurements were performed with a Cembureau constant head permeameter on cylindrical concrete specimens with or without steel bars. Since gas transfer into concrete depends on the rate of saturation of the material, the specimens were tested at different degrees of saturation: 0%, 6%, 30%, 60%, 80%, 90% and 100%. The analysis quantifies the impact of the defects created by the steel bar for each state. The results show that material composed of concrete and reinforcement can be divided into two distinct permeability zones: the plain concrete and the steel-concrete interface with or without cracking. These two zones can be associated in series and/or in parallel according to the configuration. The consequences on permeability measurement in reinforced structures are discussed.

Keywords: Reinforced concrete, durability, transfer, gas permeability, crack.

[1] stephane.multon@insa-toulouse.fr

Highlights:

- Permeability were measured on reinforced samples for different saturation degrees,
- Steel bars embedded in concrete lead to an increase in the sample permeability,
- For high saturation degrees, the steel-concrete interface is the main transfer path,
- Cracking induced by the restrained shrinkage participate to transfer,
- Equivalent defect opening can quantify the impact of the interface on air transfer.

1. Introduction

The penetration of aggressive agents, water, chloride and other ionic species into concrete is responsible for most of its deterioration [1]–[3]. The viability of many structures depends on their concrete transport properties [4]–[6]. The permeability of a reinforced concrete and the extent to which it permits diffusion are considered as major indicators of its durability [3], [5], [7]. Fluid transport in a porous material is possible because of the presence of paths of connected porosity. In concrete, the pathways are mainly: the capillary pores of the cement paste [7]–[9]; the interfacial transition zone between cement paste and aggregate [8], [10]–[12]; and micro cracks in aggregates and cement matrix [8], [13]. Most of the research on the subject has dealt with plain concrete and mortar without reinforcement, so the effect of the presence of steel bars on the permeability of reinforced concrete has been little studied. Reinforcements lead to obtain smaller cracks opening for concrete under mechanical loading and thus to decrease permeability in damaged concrete [14]–[17]. This impact of reinforcement has to be taken into account for leakage prediction in real structures [18]. The inclusion of fibres decreases permeability properties in concrete with [19], [20] or without [21] cracks due to mechanical loading. Previous experimental works analysed the mechanical role of reinforcement on the permeability of loaded concrete. In this case, several mechanisms impact concrete permeability: the modification of porosity due to mechanical loading, the cracks occurrence and the impact of the steel-concrete interface. Small stresses lead to compaction and thus to the decrease of permeability [25] and permeability increases when cracks connectivity occurs [25], [26]. In reinforced concrete samples, steels densify the cracking and reduce the crack width due to loading. Reinforcement leads to a reduction of the flow through cracks and thus of the permeability.

However, reinforcement bars are also responsible for concrete cracking due to restrained shrinkage, even without external loading. The induced cracks and also the voids at the interface with the concrete [22]–[24] disturb the transfers in concrete, particularly close to the skin, where transfer has a preponderant effect on durability. For reinforced concrete submitted to loading, the different mechanisms acting on permeability are concomitant. To obtain precise modelling, it is necessary to distinguish the part of each mechanism: the impacts of the mechanical loading, of the induced cracks and of the steel-concrete interface. As a consequence, transfers in plain and reinforced specimens without mechanical loading have to be analysed to assess the capacity of steel-concrete interfaces to provide gas transfer paths.

If the steel-concrete interfaces are actually preferential paths of transfer and become accessible to fluids from the surface through cracking, the reinforcement cover would become unable to assume its protective role against aggression and so the steel bars could be directly exposed. The degradation kinetics of reinforced concrete becomes greatly accelerated if other phenomena do not occur (healing, precipitation). Similarly, as these steel-concrete interfaces act on the kinetics of the fluid flow, they can change the time necessary to reach the steady state of flow due to their low resistance to transfer [27], according to the design of the reinforcement in the structure. In heavily reinforced structures, the steel-concrete interfaces are numerous, have considerable area and are highly connected. Therefore, they form significant pathways for transfers, which should be considered when predicting the durability, and particularly the air tightness of such structures. This study analyses the contribution of steel-concrete interfaces to gas transfer within reinforced concrete.

The degree of saturation of concrete on site is usually very high close to water supply and in locations submitted to rainfall and is usually over 80% at 50 mm depth [28], which prevents most of the transfer in plain concrete. However, the Kelvin Laplace equation indicates that cracks with an opening greater than one micrometre are drained even at high relative humidity (99.99%). So, in the presence of skin cracking, the steel-concrete interface can easily be drained even if the saturation level of the rest of the concrete is high. Since the permeability of concrete is affected by its water saturation [5], [29]–[32], it is important to perform this study on material at different states of water saturation.

2. Objectives

The objective of this paper is to analyse the impact of the steel-concrete interfaces on reinforced concrete permeability, by inducing pathways for gas transport into concrete. They can change the transfer kinetics and the time to reach steady state during a measurement of gas leak rate and can thus constitute weak zones regarding the air tightness of reinforced concrete structures. Three specific points are particularly highlighted:

- Impact of the steel-concrete interface on permeability,
- Impact of the steel-concrete interface on flow kinetics,
- Impact of induced cracking close to the steel-concrete interface on permeability.

The first two points will lead us to identify the different zones of permeability in reinforced concrete, including the steel-concrete interface and induced cracking. The third point concerns an analysis of the impact of the crack opening on the transfer. To obtain a more relevant identification and characterization of the variation of permeability with the length of the steel-concrete interfaces in site conditions, all three studies were performed for various states of saturation.

3. Theoretical background

Permeability is defined as the ability of a material to allow fluids to pass through it under a pressure gradient. This property governs the flow rate of a fluid through a porous medium. The coefficient of permeability k_a is defined by Darcy's law.

For the sake of simplicity, the "coefficient of permeability" is referred to simply as "permeability" in this article unless otherwise noted. The gas permeability of a porous solid is calculated using the Hagen-Poiseuille relationship for laminar flow of a compressible fluid through a porous medium with small capillaries under steady-state conditions. The relationship solved for the apparent permeability k_a can be written as in Eq. 1 [33].

$$k_a = \frac{2\,\mu\,L\,Q_O}{S}\frac{P_O}{{P_I}^2 - {P_O}^2} \quad \text{(Eq. 1)}$$

where Q_O is the volume flow rate of the fluid (m^3/s), S is the cross-sectional area of the specimen (m^2), L is the thickness of the specimen in the direction of flow (m), μ is the dynamic viscosity of the fluid at the test temperature (Pa.s), P_I is the absolute inlet pressure (Pa), and P_O is the outlet pressure (the pressure at which the volume flow rate is determined, assumed in this test to be equal to atmospheric pressure – N m^{-2}).

For dried air at a temperature of 20°C, the dynamic viscosity μ may be taken as $1.83e^{-5}$ Pa.s.

4. Materials and methodology

4.1. Experimental setup

The permeability of porous materials can be evaluated through a gas flow measurement using a permeameter with constant head (the difference in pressure is fixed during the measurement) or variable head. In this study, a constant head permeameter was used. The apparatus is known as a Cembureau permeameter. The permeating medium was dried air. Fig. 1 gives an overview of the apparatus. The main elements are: an air supply cylinder fitted with a pressure reducing valve, a precision pressure regulator, a pressure gauge, the permeability cell, a flow meter and a computer to record the air flow.

In order to reach a precision of 1% in the determination of permeability, Kollek's specifications [33] were followed: the inlet pressure, P_I, to the cell was controlled over a range of absolute pressure from 2 to 5 bars (2×10^5 to 5×10^5 $N.m^{-2}$) by the pressure regulator and the set pressure level was maintained within 1% of the selected pressure during the whole time of air flow measurement. The graduations on the pressure gauge were 5×10^{-2} bars (5×10^3 $N.m^{-2}$). The permeability cells were sealed by a tightly fitting polyurethane rubber joint under a pressure of 8 bars (1.5 times the maximum inlet pressure) against the curved surface. So a pressure difference of up to 4 bars (4 x 10^5 N.m^{-2}) could be applied to the specimens in the permeability cells.

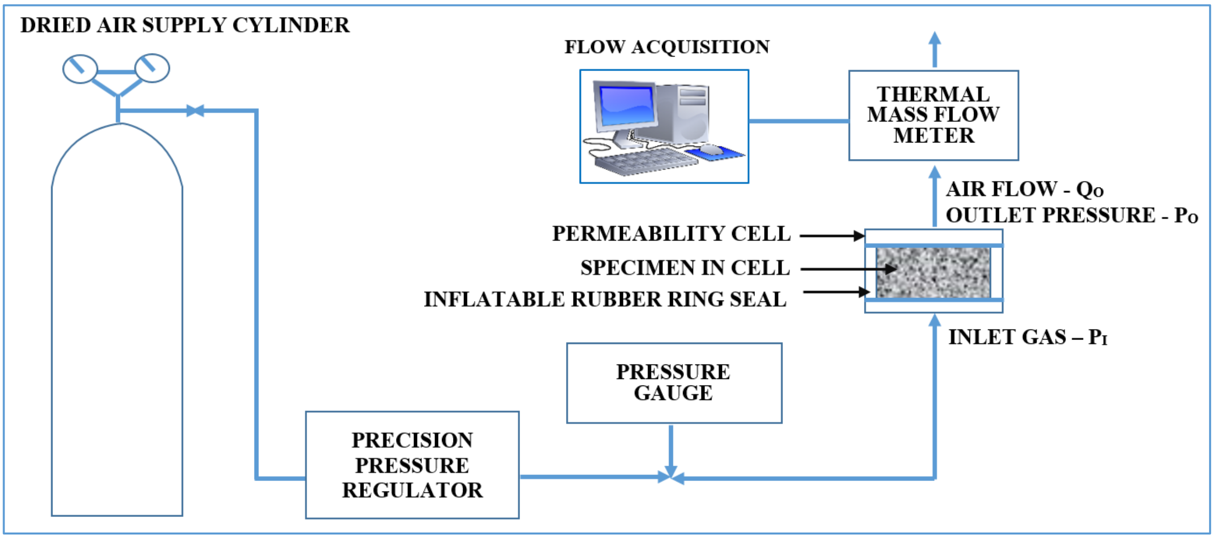

Fig. 1: Experimental apparatus

The air flow was recorded every 15 seconds by the digital thermal mass flowmeter (Brooks Instrument Hatfield PA 19440 USA, Brooks S/N: F23889 008 Model: 0254AB2B11A) to determine the air flow rate through the specimens with reliable accuracy. Two flowmeters were used according to the flow range: the first one for flows lying between 0 and 10 cm^3/min and the second one for flow between 10 and 100 cm^3/min. After initiating the percolation of dried air through the specimen at a given applied pressure, sufficient time was allowed for steady state flow to become established. The steady state condition was verified with the curves of air flow versus time. In this study, the time to reach steady state (TRSS) was short due to the transfer thickness (50 mm) [34]. The measurement allowed the TRSS to be compared among test configurations (comparison of the impact of steel bar length in concrete on TRSS) by direct comparison of the downstream flow. After having measured the flow in the steady state, the permeability k_a was calculated from the Hagen-Poiseuille equation for laminar flow of a compressible fluid through a porous body under steady state conditions (Eq. 1).

4.2. Experimental program

Different configurations can be used to measure the air flow through reinforced concrete specimens. The transfer into the accessible pores and/or into cracks of the material can be analysed with the specimen configuration illustrated in Fig. 2. In this arrangement, the concrete around the reinforcement and/or the crack openings directly governs the measured air flow and the contribution of the steel-concrete interface to the outlet flow, Q_O, cannot be isolated.

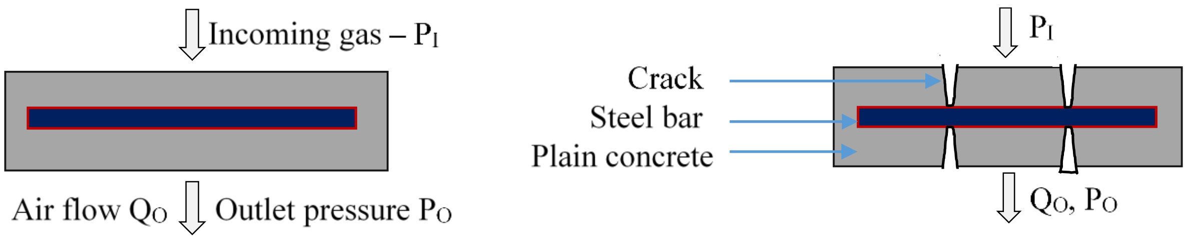

Fig. 2: Reinforced concrete for Q_O measurement: case n°1

On site, the steel-concrete interfaces can be directly or partially accessible to aggressive agents, particularly because of the presence of cracks induced, for example, by drying shrinkage or by external loading. An appropriate test setup for characterizing the impact of the steel-concrete interfaces would directly expose the steel-concrete interfaces to the inlet pressure as shown in Fig. 3.

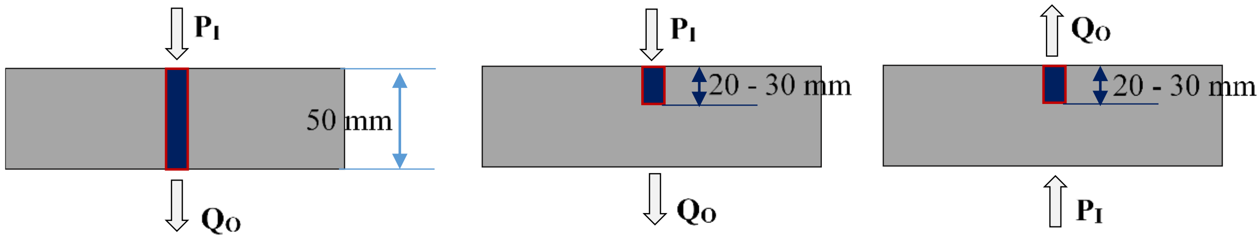

Fig. 3 Reinforced concrete for Qo measurement in this study: case n°2

During the programme, four types of sample were tested (Fig. 4):

- Plain samples (P),
- Reinforced concrete with steel bar length of 20 mm (R2),
- Reinforced concrete with steel bar length of 30 mm (R3),
- Reinforced concrete with steel bar crossing the sample from face to face (length of 50 mm, R5).

The lengths of the reinforced bars in the samples were chosen in accordance to the concrete aggregate size (16 mm). The impact of reinforcement on permeability was studied for different degrees of saturation: 0%, 6%, 30%, 60%, 80%, 90% and 100%. The degree of saturation is indicated at the beginning of the specimen reference when necessary (Fig. 4).

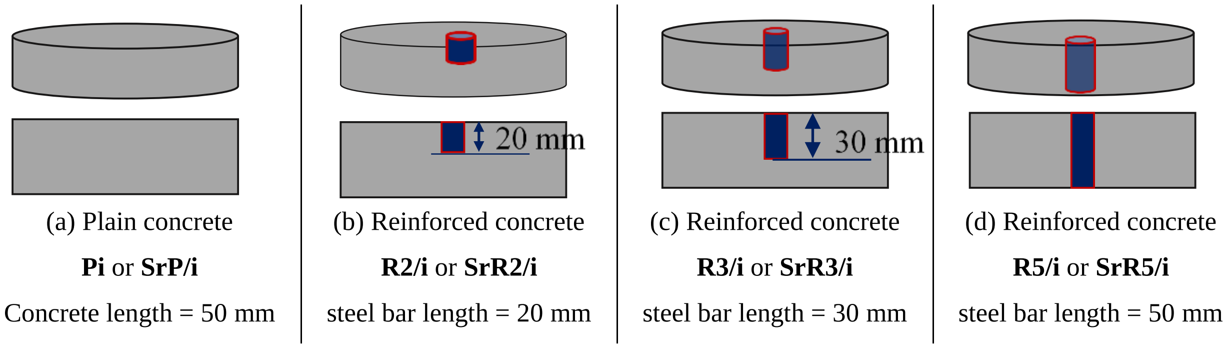

- Sr is the degree of saturation; i identifies the specimen: i =1; 2; 3.

Fig. 4: Types and codes of specimens

4.3. Samples

To limit causes of scatter, all the samples were extracted from four cylindrical specimens with a diameter, Ø, of 150 mm and height, h, of 200 mm: one specimen for the three plain samples (SrP/1, SrP/2, SrP/3) and three specimens for the reinforced concrete samples (SrR2/i, SrR3/i, SrR5/i) as shown in Fig. 5. All measurements were performed on three (3) samples of each type.

Fig. 5: Description of the samples SrP/i, SrR2/i, SrR3/I and SrR5/i

4.4. Concrete mix, casting, curing and preconditioning

Concrete mix is given in Table 1. Siliceous limestone aggregates were used. Silica contents of aggregates were about 80 and 5% for the sand and the gravels, respectively. Specimens (ϕ=150 mm, h= 200 mm) were cast in plastic moulds. Twenty-four hours after casting, they were removed from their moulds and cured in lime water at a temperature of 20 ± 2 °C for at least 60 days. This long time (60 days) in water was required to obtain a stabilized material regarding cement hydration [35]. Lime water allows an increase of the pH and a limitation of carbonation and calcium leaching [36], [37]. After curing, the samples (ϕ=150 mm, h=50 mm) were sawn from the original specimens and the first 25 mm of both sides were removed to avoid skin effects (Fig. 5). The samples were then saturated with water under vacuum and dried to obtain the different water contents. The degrees of saturation were calculated with the porosity obtained at the end of the drying process.

Table 1. Concrete mix for 1 m^3

Constituents	[kg]
Sand 0/4 rec GSM LGP1	830
Gravel 4/11 R GSM LGP1	445
Gravel 8/16 R BALLOY	550
Cement CEM I 52.5 NCE CP2 NF	320
Plasticizer SIKAPLAST TECHNO 80	2.4
Water	213

Table 2. Preconditioning description

Sr (%)	Temperature (°C)	Drying time (day)	Cumulative mass loss (%)
90.	20.	0.8	0.8
80.	40.	1.	1.6
60.	50.	1.	3.1
30.	60.	5.	5.9
6.	60.	22.	7.8
0.	105.	2.	8.2

The preconditioning of the samples is described in Table 2. The specimens of concrete were dried at four temperatures to reach the different degrees of saturation (Sr). They were first dried in an oven at 40°C to achieve Sr equal to 80%, then at 50°C to reach Sr of 60%, then at 60°C to reach 30%, and again at 60°C to achieve the smallest saturation for this temperature (considered to have been obtained when constant mass was reached, with a mass loss lower than 0.05% in 24 hours). These three temperatures were used to decrease the risk of inducing thermal cracking associated with drying at 105°C. If 105°C is considered as the reference temperature at which the degree of saturation is assumed to reach zero, the specimen "dried" at 60°C actually contained an amount of water corresponding an Sr of 6%. The saturation degree of 6% was studied to obtain the permeability at the lowest saturation degree and to minimize the impact of thermal damage. Finally, to achieve a fully dry state, samples were dried in an oven at 105°C until constant mass was reached (less than 0.1% change in mass in 24 hours). At each drying state, the samples were wrapped in aluminium foil and put into the oven to allow the moisture to spread evenly in the material. The duration of homogenization was at least equal to the drying time and the temperature was the same as during drying. The permeability test was performed after each drying stage. This preconditioning to ensure an identical material before and after drying was inspired by the literature [31], [38], [39]. For saturation at 90% and 100%, no oven drying was required. For the degree of saturation of 100%, permeability tests were performed directly at the end of the curing period in lime water. For 90%, samples were simply left in the test room at 20°C for 20 hours. The specimens were weighed before and after the permeability measurements. No variations were noted. Global degree of saturation was constant during the permeability measurement.

4.5. Concrete properties

Tables 2 presents the porosity of samples according to the configuration. The porosity accessible to water of each type of specimen and the apparent density of plain concrete are noted with the standard deviation. This porosity was determined according to the AFPC-AFREM method [40] on the complete sample including the steel bar.

The steel bars used were ribbed bars 14 mm in diameter. The ribbing of the steel surface was expected to increase adherence and reduce the voids along the steel-concrete interface.

Table 3. Concrete properties

Porosity **P** [%]	18.8 ± 0.1
Porosity **R2** [%]	19.3 ± 0.3
Porosity **R3** [%]	19.4 ± 0.2
Porosity **R5** [%]	18.8 ± 0.2
Apparent volumetric mass, **P** [kg/m^3]	2107.3 ± 3.8

As shown in Table 2, the porosity was rather high and of the same order of magnitude for all the specimens. The presence of different volumes of steel within the samples could have changed the porosity. As steel bars are non-porous, with a good quality steel-concrete interface, the transition from P to R2 and R5 could have led to a decrease of porosity. Conversely, a poor quality steel-concrete interface could have led to increases in porosity between P and R5. In this study, no significant differences were observed and no conclusions can be drawn with respect to the interface quality.

5. Results

5.1. Reproducibility of the curves of air flow

The steel-concrete interfaces and cracking resulting from restrained shrinkage around the reinforcement can be the origin of heterogeneities in reinforced concrete, which lead to differences in TRSS, so it was important to verify the reproducibility of flow measurements in the presence of reinforcement. For this purpose, each test was performed three times on one sample of each of the four configurations under study (Fig. 4). The results presented here were obtained on the samples in the driest state: 0P1, 0R2/2, 0R3/2 and 0R5/3. The samples were taken at random. Two reproducibility tests were performed: one related to measurements, starting from the same face, and one related to the impact of the choice of measurement face. The presence or absence of the steel bar on the face exposed to inlet pressure could have an impact on the measurement. The curves of air flow versus time Q(t) are shown in Fig. 6.

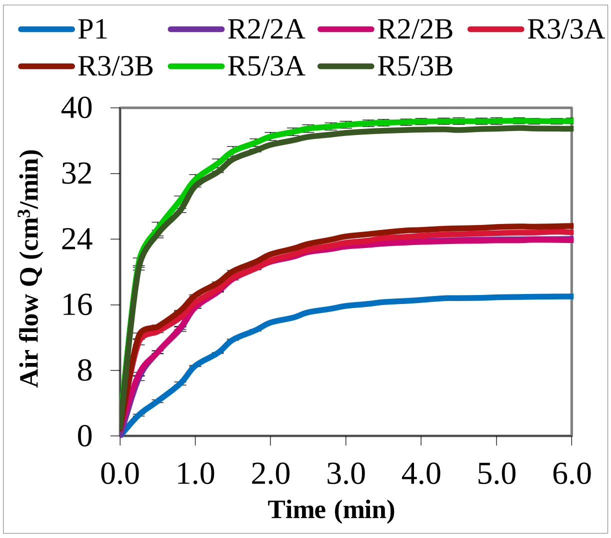

Fig. 6: Air flow Q(t) – two faces (A and B), tested at the saturation degree equal to 0% for the absolute pressure P_I equal to 2 bars (the curves corresponding to R2/2A and R2/2B coincide; the differences were lower than 0.3% of the scale)

Table 4. Maximum coefficients of variation for air flows obtained for 3 measurements on the same sample starting from a same face

(%)	P	R2	R3	R5
CoV	0.5	0.1	0.3	0.9

In all cases, the standard deviation for three measurements on the same sample was very low (less than 1% – Table 4) and the measurement was reproducible with the presence of steel bars. The volume flow rate and flow kinetics were the same whatever the face exposed to the inlet absolute pressure (Fig. 6), even for asymmetrically reinforced samples (cases of R2 and R3 in which the steel does not cross the sample completely). In the rest of the paper, no distinction will be made between the faces subjected to the inlet pressure. The results presented here for one sample of each type are representative of all the samples, even those made of reinforced concrete. Differences in amplitude could be obtained among samples in the same configuration due to the heterogeneity created at the interface by the reinforcement. It is important to note that all the curves of air flow obtained on the reinforced samples can be divided into two parts (Fig. 6):

- an initial abrupt increase in flow. This jump is greater when the length of steel in the sample is greater (R5 and R3),
- followed by the usual kinetics of fluid flow through plain concrete.

The plain samples showed no abrupt increase at the beginning but only the usual kinetics, as expected.

The initial flow jump was due to the steel-concrete interface, which represented a defect regarding the transfer of gas into reinforced concrete (discussion in section 5.3). It is important to mention that this jump is not the same as the flow peak presented by Verdier and al. [34], which corresponds to a measurement artefact due to the initiation of the inlet pressure and can be explained by the evacuation of an outlet overpressure when inlet pressure is applied. To eliminate this parasite, the pressure was always evacuated at the beginning of measurement by opening the valves at the outlet of the permeability cell. Based on Verdier and al.'s work [34] and on the measurements performed in the present work, fifteen seconds after application of the inlet pressure was enough to evacuate this overpressure. The initial time (zero date) of the air flow measurement was taken from the moment when this overpressure was evacuated.

The experimental results presented in Fig. 6 are in contrast with the measurements of porosity, which did not show any significant differences (Table 3). The difference was due to a preferential pathway of gas transport into reinforced samples that was not sufficiently significant to show an impact on porosity but was revealed by flow measurements. This shows the good sensitivity of such measurements for detecting small defects that can impact the concrete durability without significant consequences on other properties. The highest permeability of the reinforced specimens (Fig. 7) could be explained by the highest pore connectivity with the creation of preferential paths of gas transfer into the concrete near the reinforcement or the steel-concrete interface. In the case of R5, the path could be totally constituted by the steel-concrete interface, which opened out. In the case of R2 and R3, the presence of the steel bar could be the cause of cracking induced by drying in the concrete part under the steel bars. Such cracks were connected to the steel-concrete interface and could form a path between the two faces of the sample. The consequence was an increase in the air flow. The aggregate size had probably an impact on the connectivity of the pore network under the steel bars. Permeability measurement on samples with concrete thickness larger than 30 mm under the steel bar could exhibit a decrease of the initial flow jump.

5.2. Impact of steel-concrete interface on permeability

The permeability of samples was calculated from the flow rates in the steady state (Eq. 1). Fig. 7 shows the evolution of apparent and relative permeability as a function of saturation. The inlet pressure was 2 bars. The results presented were similar at all test pressures (2, 3 and 4 bars).

As usual, the relative permeability was obtained from the ratio of the permeability at a given state of saturation and the permeability at saturation state Sr = 6%: $k_{a,rel} = k_{a,Sr}/k_{a,Sr\,=\,6\%}$. The state Sr = 0% (drying of the material at 105°C) was not kept as the reference in order to limit the impact of damage due to this high temperature on the values of relative permeability. Average values and standard deviation were obtained from SrP1, SrP2, SrP3 (values in blue), SrR5/1, SrR5/2, SrR5/3 (green), SrR2/1, SrR2/2 (in purple), SrR3/1, SrR3/3 (red). Only the values of one sample (SrR2/3) were not taken into account as the measured air flow was much too high – three hundred times greater than the other values – and so was not representative.

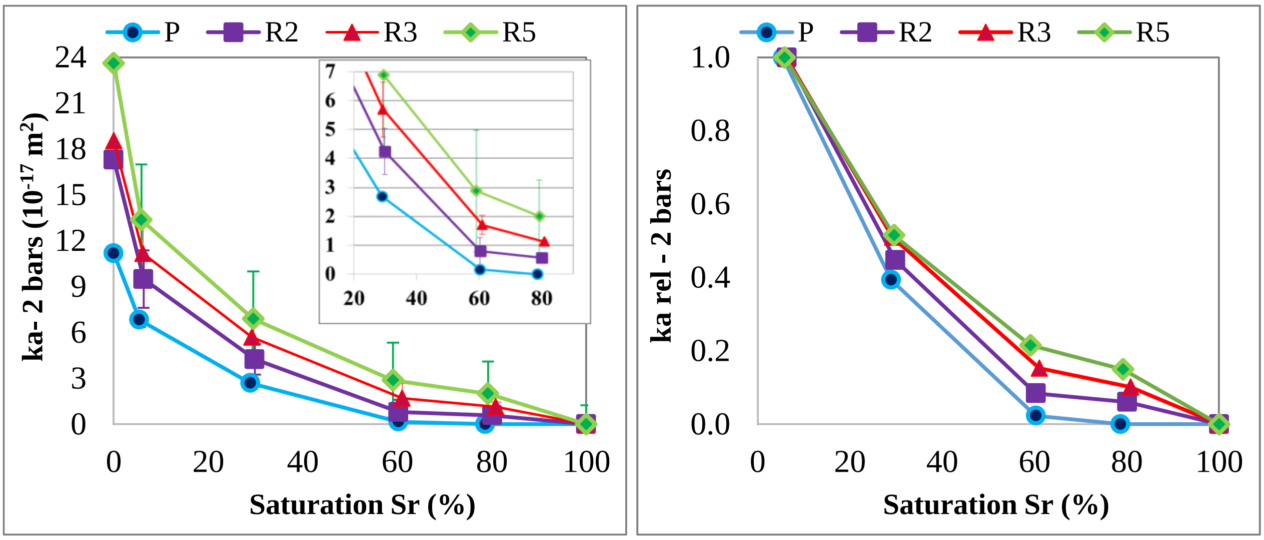

(a) (b)

Fig. 7 : Apparent permeability (a) and relative permeability $k_{Sr}/k_{Sr\,=\,6\,\%}$ (b) for $P_I = 2$ bars

Whatever the state of saturation, the permeability of plain concrete samples P was always the lowest (Fig. 7). The presence of reinforcement led to significantly increase the permeability of samples. The permeability of reinforced samples R5 (reinforcement crossing the sample) were the highest, while the values of permeability obtained for R2 and R3 (steel not completely crossing the sample) were intermediate. The zones with high permeability (preferential paths of gas transfer into the concrete near the reinforcement or steel-concrete interfaces) were more noticeable at high saturation. The presence of water in pores makes difficult the transfer of air in concrete. Air flow decreases with the increase of concrete saturation [5], [32], [41], [42]. This phenomenon depends on the geometry of the percolation path. Path with an opening greater than one micrometre can be drained even at high relative humidity (99.99%). Thus, path formed by steel-concrete interface can be drained more easily than usual concrete porosity. For Sr lying between 60% and 80%, all three reference samples P were impermeable to air (low or zero permeability as obtained by many researchers [5], [32], [41]) while all reinforced samples (R2, R3 and R5) were permeable (Fig. 7-b). This means that the pathway formed by the interface and the cracks was larger and more connected than the usual concrete pores. Consequently, they were desaturated even with the drying at 40°C, while the rest of concrete was still in a high saturation state that did not allow gas transfer. At high levels of saturation, such pathways had a greater impact on the gas transfer into the material.

Concerning the impact of the reinforcement, it is important to note the high standard deviation that can be seen in the case of the reinforced samples completely crossed by steel bars while plain concrete samples show little scatter (Fig. 7-a). This highlights the impact of the defect on flow paths. These large standard deviations of the permeability of reinforced samples can be explained by the heterogeneous nature of the steel-concrete interface [36], which can vary greatly from one sample to another according to casting (vibration), drying, and difference in verticality of the steels in the concrete during casting.

In summary, the analysis of the results presented in Fig. 7 leads us to break the downstream air flow (from which the apparent permeability is calculated) down into two distinct contributions: one zone of high permeability due to the "defect" caused by the presence of the steel/concrete interface and induced cracking, and one zone of plain concrete. In all cases, the defect is located in the vicinity of the steel. The impact is characterized by an initial jump in the measured air flow and leads to an increase of the permeability of reinforced samples.

5.3. Impact of steel-concrete interface on air flow and on flow kinetics

5.3.1. Air flow, Time to Reach Steady State (TRSS) and different permeability zones

The analysis of the kinetics of air flow is necessary to identify and quantify the impact of the presence of reinforcement on gas transfer. Fig. 8 shows the flow kinetics according to the degree of saturation Sr = 80%, 60%, 30% and 6% for one sample of each type (SrP1, SrR2/2, SrR3/3 and SrR5/2). The absolute pressure of the test was 2 bars. At Sr = 80%, no flow was measured through the reference samples, as illustrated by 80P1 in Fig. 8, while flows appeared through all the reinforced samples for this same saturation degree. For reinforced samples, the flow was almost immediate and constant. The flow rates observed through reinforced samples were due to high-permeability zones since plain concrete is not permeable at this saturation degree (Sr = 80%). This zone is called a "defect" in the following.

It is very interesting to observe that the flow through reinforced samples reached steady state almost instantaneously after application of the inlet pressure: the TRSS was less than 1 minute. This short time is representative of a medium with very low resistance to the flow (for example, concrete with serious damage, because the defects oppose little resistance to transfer). The poor adhesion between the concrete and the steel bar, and cracks in the concrete near the steel bar led to very low resistance to gas transfer and a flow rate proportional to the defect. If the adhesion was perfect, flow rates of all reinforced concrete would be zero. The presence of this defect can also be expected to modify the concrete transfer properties around the reinforcement during drying. The concrete located in the vicinity of the defect is preferentially drained by its connection to the defect.

At Sr = 60%, very low air flow was measured in the reference samples (Fig. 8). The flow was smaller than any of the flows through reinforced samples. Initial abrupt increases in the flow were observed for all the reinforced samples (R2, R3 and R5). The jumps were observed 15 seconds after the start of measurement while the flow through the plain concrete was zero. Unlike the previous state (Sr = 80%), the steady state took longer to become established in reinforced samples at Sr = 60%. The times to reach steady state of reinforced samples increased from 1 minute to 40 minutes when Sr changed from 80% to 60%. At Sr = 80%, the TRSS was very small because it was due to transfer in the defect only (which is very fast) since transfer in concrete was still zero. But at Sr = 60%, the TRSS was relatively long for the plain sample (more than 40 min), because the connectivity of the concrete percolating network was reduced by the presence of water and its tortuosity was increased. Local pressure variations can be more difficult to clear out and impact TRSS. In reinforced samples, the contribution of the concrete could be measured after the initial jump [8] and the TRSS increased due to the slow transfer in concrete as in the plain sample. Nevertheless, it was still the defect that mainly controlled the gas transfer into the material at Sr = 60%.

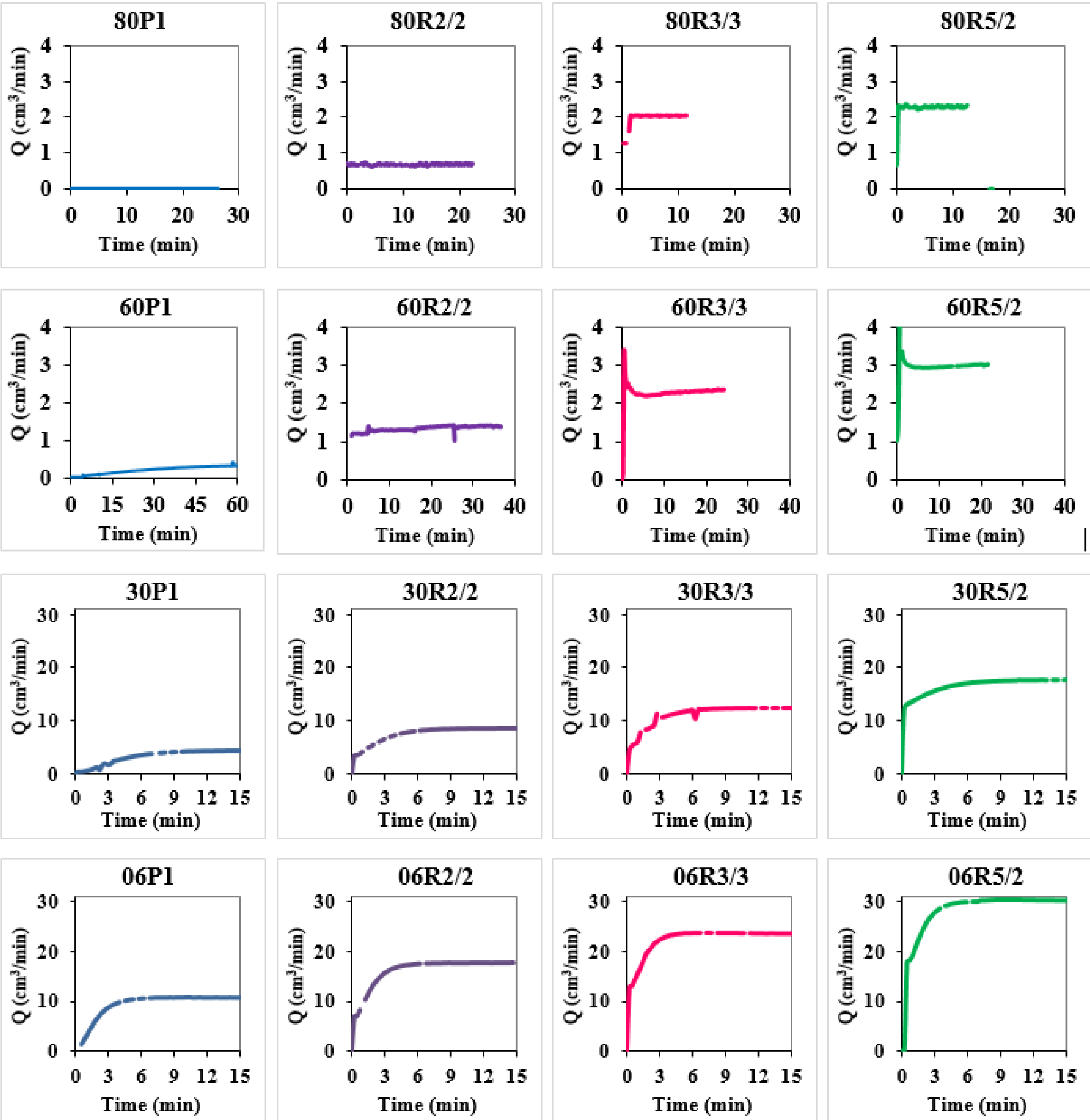

Fig. 8: Air flow kinetics and Time to Reach the Steady State at Sr = 80%, 60%, 30% and 6%

At Sr = 30% and 6%, the pores of the concrete were almost free of water, the air molecules thus encountered less resistance to their movement in the concrete pores and the TRSS decreased compared to the state Sr = 60% . However, although the TRSS of the reinforced samples for Sr lower than 30% were lower than the TRSS for Sr = 60%, they remained higher than the TRSS for Sr > 80%. In this case, water was not the only factor responsible for the resistance to flow in pores; pore tortuosity and connectivity also had a greater impact.

The variation of the air flow rate with the saturation degree for the reference sample P (in blue) was as usual for such measurements [34]. For reinforced samples, the concrete contribution was apparent after the first jump. Concerning the first jump, the longer the interface was (from R2 to R5), the greater was the jump. This was verified for all degrees of saturation, thus confirming the importance of the steel/concrete interface for air flow in reinforced concrete. Permeability tests performed on concrete thicknesses less than twice the maximum size of the aggregate could be impacted by the contribution of the interfacial transition zone (ITZ – aggregates-mortar interfaces) to transfer. The 20 or 30 mm of concrete under the reinforcement (R2 and R3 samples) did not create the same resistance to transfer as in the case of plain samples; it participated in the flow associated with the defect. The residual thickness of concrete under the reinforcement did not provide a representative volume in terms of permeability measurement. The consequence could be a preferential path linking steel/concrete interfaces and interfacial transition zones of aggregate in the concrete under the reinforcement, which would amplify the impact of the defect. However, this thickness was of the same order as that of the concrete cover in many real structures.

5.3.2. Concrete contribution to air flow kinetics

To analyse the contribution of concrete to the air flow through reinforced samples, the air flow corresponding to the contribution of the interface and cracks (referenced Q_1) was subtracted from the curve. In order to determine the flow Q_1, the plain concrete curves were first subtracted from the reinforced concrete curves. As shown in Fig. 9, the result of the subtraction, Q1, was quite constant after 30 seconds of measurement.

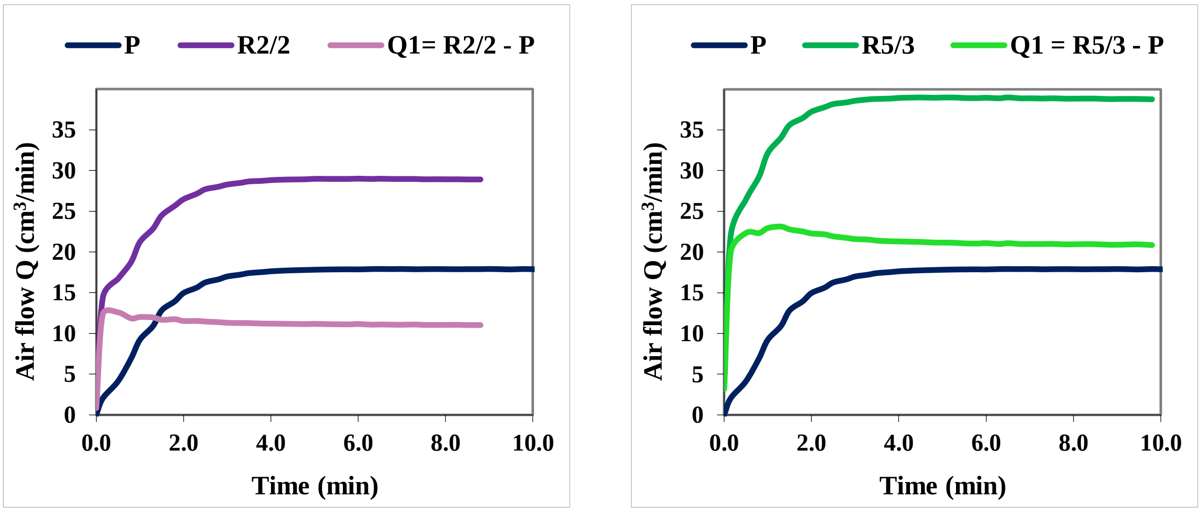

(a) (b)

Fig. 9: Air flow Q(t) – calculation of Q_1 (Sr = 0%)

Constant flows Q_1 were subtracted from the curves of reinforced samples for the samples at saturation degrees lying between 0 and 30% (Fig. 10). For the high saturation degrees (60% and 80%), the contribution of the plain concrete was low or negligible and the representation was not useful.

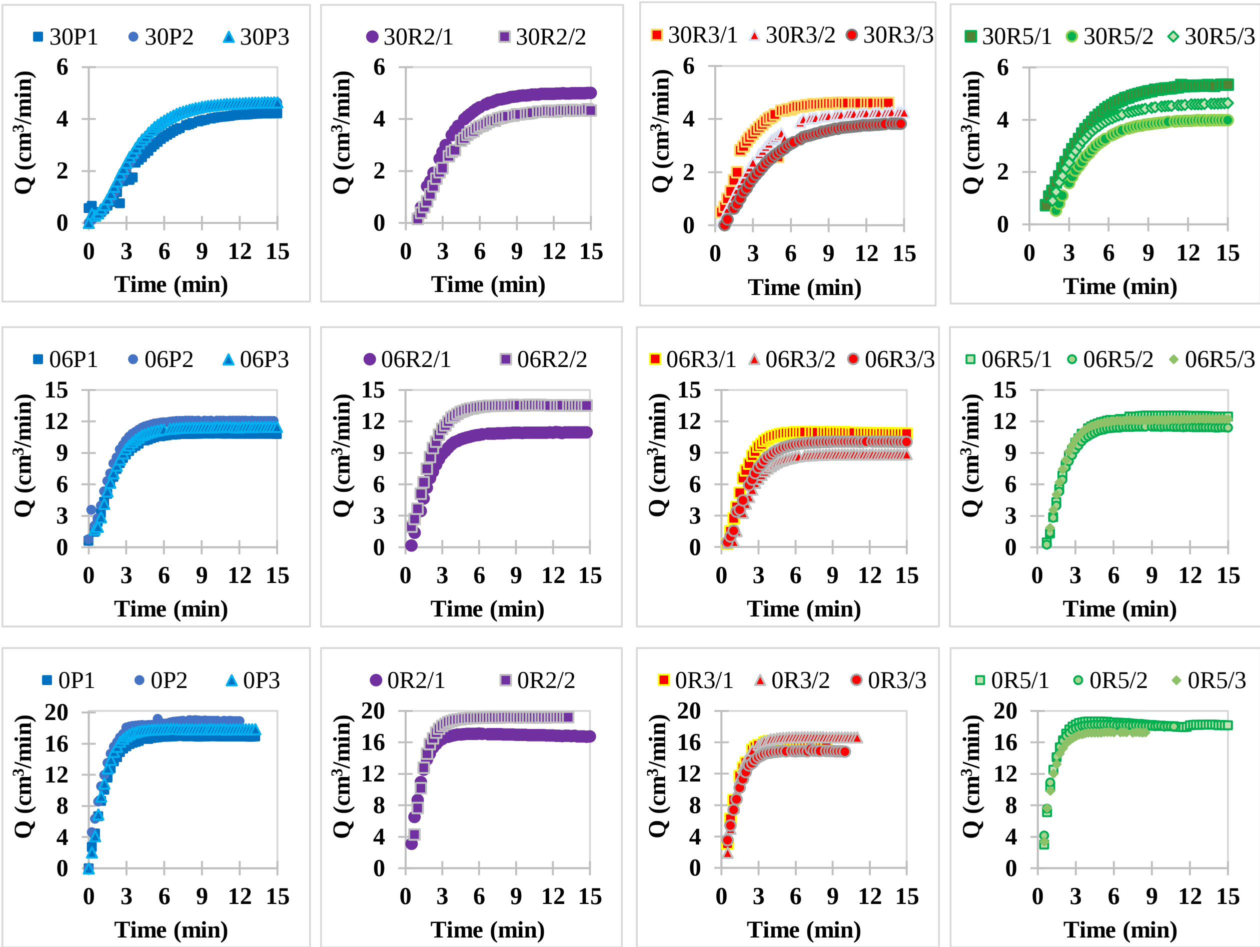

Fig. 10: Correction of curves for all samples for Sr = 0%, 6% and 30%

After the subtraction of the initial jump, all the air flows had the same kinetics (Fig. 10). The corrected curves are representative of the contribution of the sound concrete to transfer whatever the depth of reinforcement. This confirms that the beginning of the curve of air flow Q(t) is highly representative of the defect due to the interface and induced cracks. The slight differences observed in flow kinetics after subtraction (Fig. 10) may be due to the heterogeneity of the samples, which can be high since cracks are involved in air flow through reinforced samples.

In presence of reinforcement, two mechanisms act on transfer in concrete: the air flow in the interface and induced cracks, and the usual air flow in sound concrete. The transfer in the plain concrete does not appear to be greatly affected. Modelling has to consider the two phenomena in order to be representative of concrete in real structures.

5.4. Discussion

The different permeability zones in reinforced concrete are schematized in Fig. 11. In the case of R5, the interface crosses the whole sample and links the two sample faces. It can provide a transfer pathway according to the nature of the steel/concrete interface (Fig. 11-a). For R2 and R3, the interface does not link the two faces directly (Fig. 11-b) but the previous analysis has pointed out that it can also lead to a preferential pathway between the two faces since abrupt increases in air flow were observed in all reinforced R2 and R3 samples (Fig. 8).

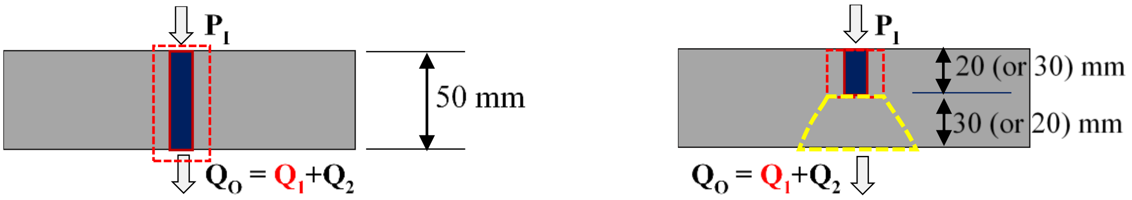

(a) (b)

Legend. $\mathbf{Q_O}$ = Total air flow; Q_2 = flow through concrete only; Q_1 = flow through the defect

Fig. 11: Permeability zones in R5 (a) and permeability zones in R2 and R3 (b)

The variation of the effect of reinforcement according to the degree of saturation can be quantified in terms of permeability (Fig. 7), in terms of relative air flows compared to the total flow Q_O (Fig. 12) or in terms of equivalent crack opening (Fig. 14). The definition of the relative air flows in Fig. 12 is:

- Q_1/Q_O, ratio between the flow due to the presence of the interface and the total air flow into the sample,
- Q_2/Q_O, ratio between the flow through the concrete and the total air flow into the sample (Fig. 12).

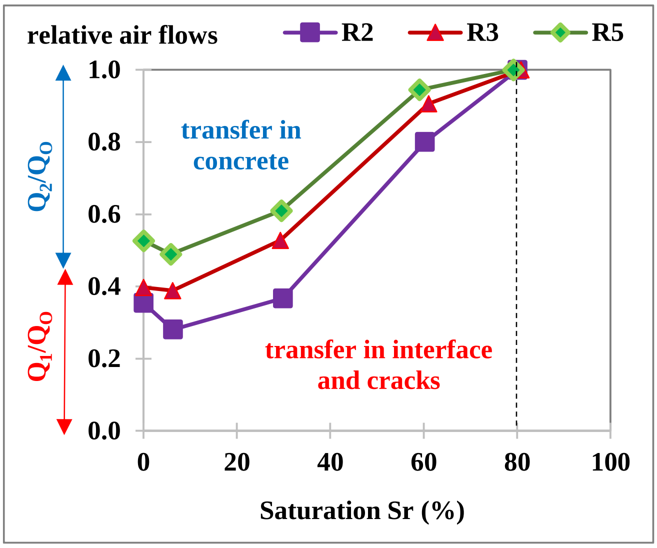

Fig. 12: Relative air flows in reinforced samples according to saturation degree

In terms of relative permeability, the impact of reinforcement was the greatest for degrees of saturation lying between 60 and 80% (Fig. 7-b). The comparison of the flows Q_1 and Q_2 confirms this result (Fig. 12): the contribution of the defect to transfer is all the more important when the saturation level is high.

These observations can be analysed in three points:

- For saturated samples (Sr equal to 100%), the whole concrete porosity and steel-concrete interfaces are filled by water and samples are totally impermeable to gas,
- At high degrees of saturation (Sr equal to 60% and 80% in the experiments), the permeability of plain concrete is still zero (Fig. 7), which is not the case for reinforced samples. This means that steel-concrete adherence is not perfect and impacts gas transfer because of its direct connection with the surface in the case of R5. In the case of the samples R2 and R3, it indicates that there is not only the pathway created by steel-concrete interfaces but also a continuity of the defect in the concrete below the steel (Fig. 11-b), which can be induced by the presence of cracks and by pathways through interfacial transition zones of aggregates. In high states of saturation, the steel-concrete interfaces and induced cracks are thus the main transfer vector in reinforced samples (Fig. 12). This result has an implication for the durability of structures: the concrete in situ is generally subjected to high levels of water saturation [43], and the percentage of transfer through concrete skin by cracks could be particularly high compared to transfer through concrete (Fig. 12). It could be the main mechanism to be considered for transfer through the concrete skins of structures.

- At low degrees of saturation, the pores of the concrete surrounding the reinforcement are gradually emptied of water, which increases the contribution of concrete to the air flow (Fig. 12). Moreover, the impact of concrete shrinkage on transfer is amplified. The shrinkage induced by drying is restrained by the rigid inclusion of the steel bar in the reinforced samples, where it leads to tensile stresses in the concrete and to cracks. Consequently the pores can be connected to the cracks and to the steel-concrete interface, the consequence being an increase in gas transfer. These cracks were already present in reinforced samples for saturation degrees between 60% and 80%. At low saturation degrees, shrinkage strains are greater and the induced cracks grow, thus possibly increasing the contribution of the defect to the air flow. However, the relative contribution of a defect decreases with decreasing degree of saturation (Fig. 12): for a low saturation state, the proportion of transfer in the concrete increases faster than the contribution of the defect, except for a saturation degree equal to 0, for which the contribution of the defect increases suddenly, probably because the high drying temperature (105°C) between 6 and 0% leads to associated damage.

These phenomena contributed to the greater relative permeability of reinforced samples (Fig. 7). In order to complete this analysis, samples were observed with a video microscope (Keyence VH-5911, maximum magnification x 175). Fig. 13 shows a microscopic view of the steel-concrete interface of the sample R5/1 (magnifications x 25 for Fig. 13-a and x 175 for b).

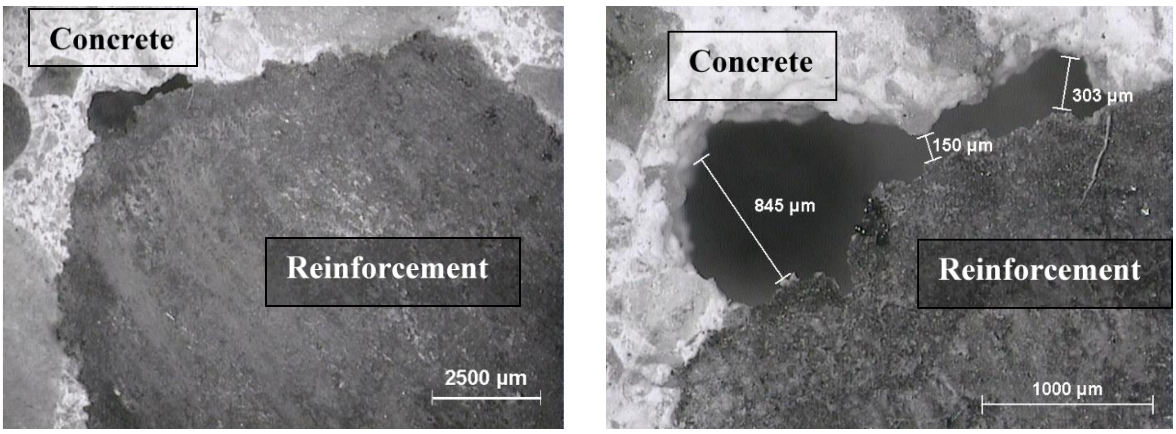

(a) (b)

Fig. 13: Detachment of the reinforcement from the concrete at steel-concrete interface

As could be expected, the geometry of the interface was very complex. The microscopic observation indicated the presence of some irregular voids in the contact between concrete and steel. The voids did not cross the sample but were localized (Fig. 13-b) as already observed by Mohammed and al. [44]. With the precision of the apparatus used here, no detachment appeared anywhere around the reinforcement (Fig. 13-a). However, detachments with openings smaller than 10 μm may exist. They would not be observable with this video microscope. The specimens would have to be sawn for more precise apparatus to be used. This was not done since it could lead to the interface being modified.

To quantify the opening necessary to obtain the measured permeability, equivalent crack openings were calculated from flows. For this purpose, the defect caused by the interface and the induced cracking was modelled as a single perfect crack with an equivalent crack opening, *w*, completely surrounding the steel bar. This opening was determined from the air flow Q_1, which characterizes the impact of the defect on the permeability. Different works propose a determination of the crack opening w from air flow [15], [17], [45]. The equation below (2) is drawn from Mivelaz's work [16]:

$$w^3 = \frac{24\,\mu\,L\,R\,TQ_1}{\xi\,\left({P_I}^2 - {P_O}^2\right)} \qquad \text{(Eq. 2)}$$

where μ is the dynamic viscosity of the fluid at the test temperature (Pa.s), P_I the inlet pressure (absolute) (Pa), P_O the outlet pressure - assumed to be equal to the atmospheric pressure (Pa) in this test, R the gas constant (J/kg/K), T the temperature (K) and ξ a flow coefficient that essentially characterizes the network tortuosity.

During the test, the evolution of the flow is characteristic of the presence of different defects. To quantify the impact of these defects on permeability, the tortuosity, the connectivity, the constrictivity of the pore network, and the interactions between cracks and concrete porosity should be taken into account. The importance of each parameter for permeability depends on the geometry of the actual percolation path which is difficult to characterize. However, the measured flow highlights the range of the impact and allows a simplified evaluation. This calculation assumes constant thickness for the defect. In order to quantify the approximation of this approach, the calculation is performed for two extreme values of the flow coefficient ξ. Thus, the impact of the geometry of the percolation path on permeability is evaluated.

This approach was chosen because it took only a few parameters (w and ξ) into account in comparison with others. According to Ripphaussen [46], cited by Mivelaz [16], the flow coefficient, ξ, is defined as the ratio of flow through cracks with an opening of w and the theoretical flow through two smooth parallel planes having the same opening, w . ξ is then less than 1 and takes the roughness and the tortuosity of the transfer path into account. The equivalent crack of width *w* is assumed to be all around the reinforcement over the entire sample thickness. Its length is equal to the thickness of the samples (L). The flow coefficient, ξ, is assumed to be constant while, in reality, the crack network is modified by drying and the coefficient could increase for the lowest saturation degree. The calculated opening is approximate and does not represent reality but it enables the impact of the opening due to steel-concrete interfaces on the concrete permeability to be analysed and compared. The defect openings thus calculated are presented in Fig. 14 for a relative inlet pressure of 1 bar and for two extreme assumptions of flow coefficient, ξ:

- A flow coefficient, ξ, of 1, which represents direct transfer [16],
- A flow coefficient, ξ, of 0.08, which represents usual transfer in a diffusive cracking pattern in concrete [16], [47].

The mean values and standard deviations presented in Fig. 14 were obtained from the values for all samples tested (except SrR2/3 as explained above).

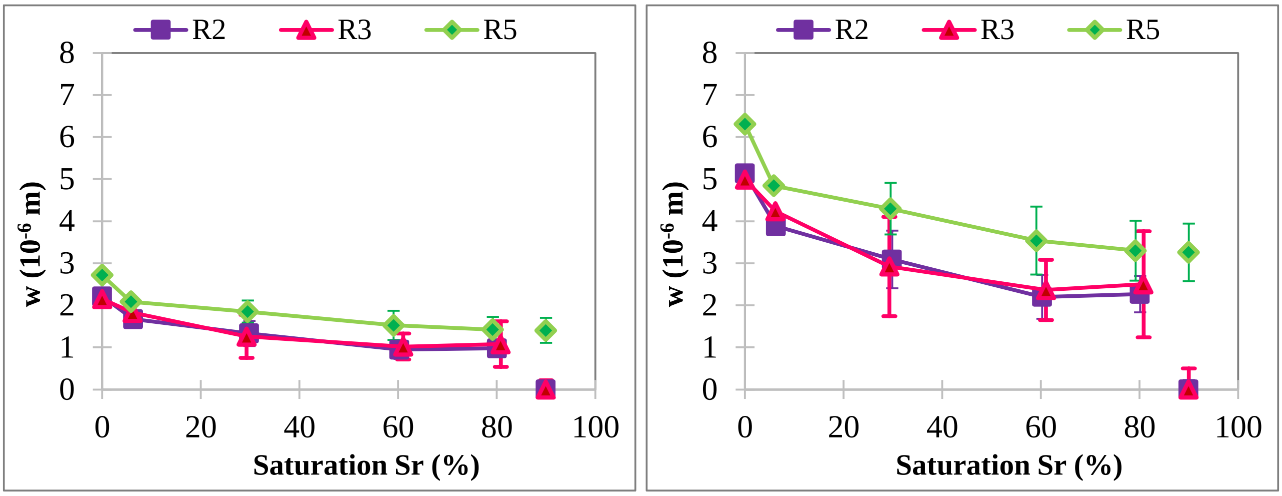

(a) (b)

Fig. 14: Defect opening, *w*, for two assumptions of flow coefficient, ξ, equal to 1 (a) and 0.08 (b)

Between 0 and 80% of saturation, two slopes can be distinguished in the variation of the defect opening *w*:

- A fairly constant evolution between Sr = 80% and 6%
- A marked change of gradient for the last drying between Sr = 6% and 0%.

This change for the lowest saturation degree could be due to notable damage occurring in the concrete during the drying at 105 °C. The increase of the calculated opening *w* presented in Fig. 14 globally quantifies the increase of transfer properties of the defect with drying. In reality, it may be partially due to the increase of the opening but it is probably also due to the movement of water out of the cracks and to the increase in crack connectivity, all of which all make transfer easier in the samples.

All the calculated values of opening *w* are close and lie below 7 µm whatever the assumptions on the flow coefficient, ξ (Fig. 14). Unlike the localized voids observed under the microscope (Fig. 13), which did not cross the samples, the calculated detachments had to cross the samples to obtain the flows measured during permeability tests. No measurement was performed between 100% and 80% with the same preconditioning of samples. As defects with openings greater than 1 µm are drained at very high relative humidity (up to 99%, Kelvin Laplace equation), the air transfer in interfaces (and in cracks) could be expected to be between 80% and 99% for such openings. In reality, it depends on the morphology of the pathways. If there are only pathways with large openings (greater than 1 µm), a sample should be permeable even at very high degrees of saturation (higher than 95%) but, if the defect is composed of several pathways with smaller openings (less than 1 µm), it can become airtight for lower degrees of saturation. Consequently, to complete the evaluation of the pathways in the different samples, another degree of saturation was studied. For this purpose, samples were initially saturated with water under vacuum and then stored in an air-controlled test room (RH of 60% and temperature of 20°C) for only one day. The objective of this additional preconditioning was to drain only the defects, such as the steel/concrete interface, but to keep the percolating network of the concrete full of water. In these conditions, the concrete sample was still wet even if its surface was slightly dry. The global saturation rate of these samples is about 90% after this preconditioning. The permeability test was then performed and showed that:

- the air flow through plain samples was still zero,
- the air flows through reinforced samples R2 and R3 were zero, and the equivalent opening w was thus zero for this saturation degree (Fig. 14),
- the air flow through reinforced concrete R5 was not zero and the equivalent crack opening calculated was equal to the opening obtained for 80% (Fig. 14).

Results on R2 and R3 indicate that the defects that crossed the samples at 80% no longer formed a pathway for air flow at larger saturation degrees: the concrete below the steel bar (thickness: 20 mm for R3 and 30 mm for R2) was not permeable to gas at 90% saturation and so resisted gas transfer into the material. Results on R5 show that, apart from localized voids, there was actually a connected interface between the steel bar and the concrete, which crossed the entire thickness of the samples. Its equivalent opening was effectively smaller than 5 µm and could not be seen in the microscopic analysis (Fig. 13).

The impact of reinforcement bars on permeability studied in this work should be dependent on numerous parameters (concrete composition, steel bars diameter, confinement pressure…). Concerning concrete composition, aggregate size and composition should impact the effect as it modifies the ITZ porosity [48]–[50]. Decreasing the aggregate size could lead to increase the tortuosity in the percolation paths due to ITZ and thus to decrease the connection between the external environment and steel bars. The impact of steel bars on permeability could be lower for concrete with smaller aggregate. The impact of steel bar diameters would be dependent on steel / concrete ratio. For a same volume of concrete, the volume of voids at the interface should be lower for bars with smaller diameter. It should lead to smaller modification of permeability. At the opposite, for a same steel / concrete ratio, using smaller bars would lead to increase the number of bars. Each bar should create percolation paths. It should lead to increase the global permeability. Future works should quantify precisely this effect. The confinement pressure applied to the specimen can also modify the results. In this program, six pressures lying between 3 and 9 bars were used for R5 sample (reinforcement crossing the sample) at the lowest saturation degree. As expected, no modification of the permeability was noted for plain samples. Such confinement pressures are too low to imply the reduction of the porosity. For reinforced samples, a decrease of the flow were observed for increasing pressure as the pressure leads to the closure of the interface (decrease of 6% of the permeability for pressure increasing from 3 to 9 bars). In case of damaged concrete, the application of confining pressure can decrease the opening of the existing cracks but the relative displacements of cracks lips prevent total reclosure. Decrease of flow can be expected as long as the confinement pressure does not lead to supplementary cracking.

The results presented in this paper cannot be directly extended to water permeability. Indeed, movements of water in such interfaces would lead to the combination with numerous chemical mechanisms: additional hydration of cement, precipitation of new phases, and steel corrosion according to water composition and pressure [51]. The objective of the study was to decrease such risk of interaction and future works should analyse the impact of combination between potential cicatrisation in case of water transfer.

The high flow rate observed through the defects and the increase in permeability with reinforcement emphasized the great connectivity of the pores and steel/concrete interfaces in the reinforced samples. In literature, Singh and Singhal showed the decrease of permeability with the inclusion of steel fibres in concrete for unloaded concrete [21]. For fibres reinforced concrete, the percolation path induced by the steel fibres is discontinuous and the cracks which could be induced by restrained shrinkage would be smaller than in plain concrete. Such small cracks would have little impact on permeability [19], [20]. At the opposite, the presence of usual steel reinforcement in concrete induces continuous and larger percolations paths. Such continuous paths can largely impact permeability as shown in the present study. In conclusion, small continuous defects in concrete, such as steel/concrete interfaces and small concrete skin cracks can lead to permeability twice that expected for the plain samples usually used for permeability measurements. This illustrates and quantifies the risk associated with the use of measurements on plain concrete to evaluate and predict the transfer behaviour of real structures. Modelling based on permeability obtained on plain samples should take the impact of cracks and interfaces into account to obtain more relevant calculations, particularly close to the concrete skin. The experimental programme presented in this paper can thus be used to evaluate the scatter on concrete permeability due to the presence of reinforcement.

6. Summary

Permeability characterizes the ability of materials to resist the penetration of aggressive agents. It is an important indicator of durability for structures in reinforced concrete. The presence of reinforcement affects the concrete cover and the permeability. The present study contributes the following results:

(a) The presence of steel bars embedded in concrete, in parallel with the flow associated with the inlet pressure, leads to an increase of the permeability of the composite material due to the steel-concrete interface (particularly porous) and to cracking induced by restrained shrinkage (which can be connected with the steel-concrete interface). In these interfaces and induced cracks, the transfer is accelerated,

(b) Steel-concrete interfaces modify the gas flow kinetics in reinforced concrete. For reinforced samples, tests showed that two transfer mechanisms existed: a sudden jump reflecting the effect of the steel-concrete interface and a more progressive transfer, characteristic of the permeability in concrete,

(c) At high degrees of saturation (above 60% moisture saturation), the concrete-steel interface is the main gas transfer vector in reinforced concrete; it is desaturated and connected to the surface while the concrete remains impermeable to gas. It is important to model permeability in structures subjected to a variety of environmental conditions.

(d) By representing the defect as a crack, the equivalent opening can be calculated from the air flow. The evolution of the damage of the steel-concrete interface with drying is reflected by an increase in the opening of the equivalent crack. Even small defects (equivalent opening of some micrometres) are sufficient to obtain permeability twice that measured on plain concrete. This should be taken into account in calculations used for prediction.

Finally, the present study opens up perspectives for the characterization and quantification of the geometry of the steel-concrete interface according to the type of reinforcement. For this, it will be necessary to continue the experimental programme on different types of steels and different thicknesses of samples. These studies would contribute to better predictions of the durability of reinforced concrete structures.

7. Acknowledgment

The authors acknowledge the financial support provided by the project "Non-destructive evaluation of containment of nuclear power plants" (ENDE) financed by the Programme Investissement d'Avenir (PIA – Centre National de la Recherche Scientifique, délégation Provence et Corse, France). The opinions presented in this paper reflect only those of the authors and do not necessarily represent the opinions of the funding agencies.

8. References

[1] N. T. Vu, "Contribution à l'étude de la corrosion par carbonatation du béton armé: Approche expérimentale et probabiliste," PhD thesis, Institut National des Sciences Appliquées de Toulouse, 2011.

[2] B. Lee, J. Hyun, Y. Kim, and K. Shin, "Chloride Permeability of Damaged High-Performance Fiber-Reinforced Cement Composite by Repeated Compressive Loads," *Materials (Basel).*, vol. 7, no. 8, pp. 5802–5815, Aug. 2014.

[3] L. Basheer, J. Kropp, and D. J. Cleland, "Assessment of the durability of concrete from its permeation properties: a review," *Constr. Build. Mater.*, vol. 15, no. 2–3, pp. 93–103, Mar. 2001.

[4] J.-P. Ollivier, J.-M. Torrenti, and M. Carcasses, *Propriétés physiques du béton et de ses constituants*. Hermes, Lavoisier, 2012.

[5] A. Abbas, M. Carcasses, and J.-P. Ollivier, "Gas permeability of concrete in relation to its degree of saturation," *Mater. Struct.*, vol. 32, no. 1, pp. 3–8, 1999.

[6] S. Care and F. Derkx, "Determination of relevant parameters influencing gas permeability of mortars," *Constr. Build. Mater.*, vol. 25, no. 3, pp. 1248–1256, Mar. 2011.

[7] H. Hilsdorf and J. Kropp, *Performance Criteria for Concrete Durability*. CRC Press, 2004.

[8] G. De Schutter and K. Audenaert, *Report 38: Durability of Self-Compacting Concrete - State-of-the-Art Report of RILEM Technical Committee 205-DSC*. RILEM Publications, 2007.

[9] T. C. Powers, “Structure and Physical Properties of Hardened Portland Cement Paste,” *J. Am. Ceram. Soc.*, vol. 41, no. 1, pp. 1–6, Jan. 1958.

[10] J. C. Maso, *Interfacial Transition Zone in Concrete*. CRC Press, 2004.

[11] J. P. Ollivier, J. C. Maso, and B. Bourdette, “Interfacial transition zone in concrete,” *Adv. Cem. Based Mater.*, vol. 2, no. 1, pp. 30–38, Jan. 1995.

[12] K. L. Scrivener, A. K. Crumbie, and P. Laugesen, “The interfacial transition zone (ITZ) between cement paste and aggregate in concrete,” *Interface Sci.*, vol. 12, no. 4, pp. 411–421, 2004.

[13] M. Ismail, “Etude des transferts et de leurs interactions avec la cicatrisation dans les fissures pour prolonger la durée de service des infrastructures (ponts, centrales nucléaires),” PhD thesis, Institut National des Sciences Appliquées de Toulouse, 2006.

[14] C. Desmettre, “Contribution à l’étude de la perméabilité du béton armé sous sollicitations statiques et cycliques,” PhD thesis, École Polytechnique de Montréal, 2011.

[15] U. Greiner and W. Ramm, “Air leakage characteristics in cracked concrete,” *Nucl. Eng. Des.*, vol. 156, no. 1, pp. 167–172, 1995.

[16] P. Mivelaz, “Etanchéité des structures en béton arme. Fuites au travers d’un élément fissuré,” PhD thesis, École Polytechnique Fédérale de Lausanne, 1996.

[17] S. H. Rizkalla, B. L. Lau, and S. H. Simmonds, “Air leakage characteristics in reinforced concrete,” *J. Struct. Eng.*, vol. 110, no. 5, pp. 1149–1162, 1984.

[18] P. Riva, L. Brusa, P. Contri, and L. Imperato, “Prediction of air and steam leak rate through cracked reinforced concrete panels,” *Nucl. Eng. Des.*, vol. 192, no. 1, pp. 13–30, 1999.

[19] M. Hubert, C. Desmettre, and J.-P. Charron, “Influence of fiber content and reinforcement ratio on the water permeability of reinforced concrete,” *Mater. Struct.*, vol. 48, no. 9, pp. 2795–2807, Jun. 2015.

[20] J. Rapoport, C. Aldea, S. Shah, B. Ankenman, and A. Karr, “Permeability of Cracked Steel Fiber-Reinforced Concrete,” *J. Mater. Civ. Eng.*, vol. 14, no. 4, pp. 355–358, 2002.

[21] A. P. Singh and D. Singhal, “Permeability of Steel Fibre Reinforced Concrete Influence of Fibre Parameters,” *Procedia Eng.*, vol. 14, pp. 2823–2829, Jan. 2011.

[22] T. A. Soylev and R. François, “Quality of steel–concrete interface and corrosion of

reinforcing steel," *Cem. Concr. Res.*, vol. 33, no. 9, pp. 1407–1415, Sep. 2003.

[23] W. B. Na, T. Kundu, and M. R. Ehsani, "Ultrasonic guided waves for steel bar concrete interface testing," *Mater. Eval.*, vol. 60, no. 3, 2002.

[24] T. U. Mohammed, N. Otsuki, H. Hamada, and T. Yamaji, "Chloride-Induced Corrosion of Steel Bars in Concrete with Presence of Gap at Steel-Concrete Interface," *Mater. J.*, vol. 99, no. 2, pp. 149–156, Mar. 2002.

[25] M. Choinska, A. Khelidj, G. Chatzigeorgiou, and G. Pijaudier-cabot, "Effects and interactions of temperature and stress-level related damage on permeability of concrete," vol. 37, pp. 79–88, 2007.

[26] V. Picandet, A. Khelidj, and G. Bastian, "Effect of axial compressive damage on gas permeability of ordinary and high-performance concrete," *Cem. Concr. Res.*, vol. 31, no. 11, pp. 1525–1532, Nov. 2001.

[27] J. Verdier, "Contribution à la caractérisation de l'évolution du taux de fuite des enceintes de confinement du parc nucléaire," PhD Thesis, Université Paul Sabatier, Toulouse., 2001.

[28] D. Stark, "The moisture condition of field concrete exhibiting alkali-silica reactivity," in *Durability of concrete. G. M. IDORN International Symposium*, 1992, pp. 973–987.

[29] Z. E.-A. Kameche, F. Ghomari, A. Khelidj, and M. Choinska, "La perméabilité relative comme indicateur de durabilité: Influence de l'état hydrique du béton et de la taille des éprouvettes," in *XXe Rencontres Universitaires de Génie Civil*, 2012.

[30] V. Baroghel Bouny, "Développement d'une approche globale, performantielle et prédictive de la durabilité des structures en béton (armé) sur la base d'indicateurs de durabilité : Bilan et perspectives : Caracterisation de la microstructure des bétons, étude des proprietés hyd," *Etudes Rech. des Lab. des ponts chaussees - Ser. ouvrages d'art*, no. OA 63, Dec. 2008.

[31] M. Carcassès, A. Abbas, J.-P. Ollivier, and J. Verdier, "An optimised preconditioning procedure for gas permeability measurement," *Mater. Struct.*, vol. 35, no. 1, pp. 22–27, 2001.

[32] J. P. Monlouis-Bonnaire, J. Verdier, and B. Perrin, "Prediction of the relative permeability to gas flow of cement-based materials," *Cem. Concr. Res.*, vol. 34, pp. 737–744, 2004.

[33] J. J. Kollek, "The determination of the permeability of concrete to oxygen by the

Cembureau method—a recommendation," *Mater. Struct.*, vol. 22, no. 3, pp. 225–230, 1989.

[34] J. Verdier, M. Carcassès, and J. P. Ollivier, "Modelling of a gas flow measurement: Application to nuclear containment vessels," *Cem. Concr. Res.*, vol. 32, no. 8, pp. 1331–1340, 2002.

[35] V. Waller, "Relations entre composition des betons, exothermie en cours de prise et resistance en compression," PhD Thesis, École Nationale des Ponts et Chaussées, 1999.

[36] Z. Makhloufi, E. H. Kadri, M. Bouhicha, A. Benaissa, and R. Bennacer, "The strength of limestone mortars with quaternary binders: Leaching effect by demineralized water," *Constr. Build. Mater.*, vol. 36, pp. 171–181, 2012.

[37] A. A. Ramezanianpour, A. Pilvar, M. Mahdikhani, and F. Moodi, "Practical evaluation of relationship between concrete resistivity, water penetration, rapid chloride penetration and compressive strength," *Constr. Build. Mater.*, vol. 25, no. 5, pp. 2472–2479, 2011.

[38] C. Antón, M. A. Climent, G. de Vera, I. Sánchez, and C. Andrade, "An improved procedure for obtaining and maintaining well characterized partial water saturation states on concrete samples to be used for mass transport tests," *Mater. Struct.*, vol. 46, no. 8, pp. 1389–1400, Nov. 2012.

[39] RILEM TC 116-PCD, "Permeability of concrete as a criterion of its durability, final report," *Mater. Struct.*, vol. 32, no. 217, pp. 163–173, Apr. 1999.

[40] J.-P. Ollivier, Ed., *Durabilité des bétons, méthodes recommandées pour la mesure des grandeurs associées à la durabilité compte rendu des journées techniques AFPC-AFREM.* Toulouse: Laboratoire matériaux et durabilité des constructions, 1997.

[41] Z. A. Kameche, F. Ghomari, M. Choinska, and A. Khelidj, "Assessment of liquid water and gas permeabilities of partially saturated ordinary concrete," *Constr. Build. Mater.*, vol. 65, pp. 551–565, 2014.

[42] G. Villain, V. Baroghel-Bouny, C. Kounkou, and C. Hua, "Mesure de la perméabilité aux gaz en fonction du taux de saturation des bétons," *Rev. Française Génie Civ.*, vol. 5, no. 2–3, pp. 251–268, 2001.

[43] J.- Jaccoud and P. Laurencet, "Fissuration, étanchéité et durabilité des structures en beton armé," *Ann. du bâtiment des Trav. publics*, no. 6, pp. 28–37, Dec. 2000.

[44] T. U. Mohammed, T. Yamaji, T. Aoyama, and H. Hamada, “Marine Durability of 15-Year Old Concrete Specimens Made with Ordinary Portland, Slag,and Fly Ash Cements,” in *Seventh CANMET/ACI International Conference on Fly Ash, Silica Fume, Slag and Natural Pozzolans in Concrete, SP-199*, 2001, pp. 541–560.

[45] T. Suzuki, K. Takiguchi, and H. Hotta, “Leakage of gas through concrete cracks,” *Nucl. Eng. Des.*, vol. 133, no. 1, pp. 121–130, 1992.

[46] B. Ripphausen, “Untersuchungen zur Wasserdurchlässigkeit und Sanierung von Stahlbetonbauteilen mit Trennrissen,” PhD thesis, Rheinisch-Westfälische Technische Hochschule Aachen, 1989.

[47] W. Buss, “Proof of Leakage Rate of a Concrete Reactor Building,” *ACI Spec. Publ.*, vol. 34, pp. 1291–1320, Jan. 1972.

[48] A. Elsharief, M. D. Cohen, and J. Olek, “Influence of aggregate size , water cement ratio and age on the microstructure of the interfacial transition zone,” vol. 33, pp. 1837–1849, 2003.

[49] W. A. Tasong, C. J. Lynsdale, and J. C. Cripps, “Aggregate-cement paste interface Part I . Influence of aggregate geochemistry,” vol. 29, pp. 1019–1025, 1999.

[50] A. Makani, T. Vidal, G. Pons, and G. Escadeillas, “Time-dependent behaviour of high performance concrete: influence of coarse aggregate characteristics,” *EPJ Web Conf.*, vol. 6, p. 3002, 2010.

[51] H. Ranaivomanana, J. Verdier, A. Sellier, and X. Bourbon, “Prediction of relative permeabilities and water vapor diffusion reduction factor for cement-based materials,” *Cem. Concr. Res.*, vol. 48, pp. 53–63, 2013.